Journal of Power Sources 196 (2011) 8450–8462

Contents lists available at ScienceDirect

Journal of Power Sources

journal homepage: www.elsevier.com/locate/jpowsour

Comparison of single particle and equivalent circuit analog models for a lithium-ion cell

Saeed Khaleghi Rahimian[1], Sean Rayman[2], Ralph E. White[*,3]

Department of Chemical Engineering, University of South Carolina, Columbia, SC 29208, USA

ARTICLE INFO

Article history:
Received 18 April 2011
Received in revised form 31 May 2011
Accepted 1 June 2011
Available online 12 June 2011

Keywords:
Single particle model
Equivalent circuit analog model
Nonlinear parameter estimation

ABSTRACT

The physics-based single particle (SP) model was compared to the semi-empirical equivalent circuit analog (ECA) model to predict the cell voltage under constant current charge and discharge for different sets of Li-ion cell data. The parameters of the models were estimated for each set of data using nonlinear least squares regression. In order to enhance the probability of finding the global optima, a combination of the trust region method with a genetic algorithm was applied to minimize the objective function (the sum of squared residuals). Several statistical quantities such as sum of the squared errors, adjusted R^2, root mean squared error, confidence intervals of the parameters, and prediction bounds were included to compare the models. A significance test (t test) on the parameters and the analysis of the variances (F and χ^2 tests) were also performed to discriminate between the goodness of the fit obtained from the two models. The statistical results indicate that the SP model superiorly predicts all sets of data compared to the ECA model, while the computation times of both models are on the same order of magnitude.

1. Introduction

Today several models for Li-ion cells are available. Most of these models are generally categorized into two main groups, physics-based and empirical. Physics-based models consider the physical phenomena which occur in batteries including the material and charge transfer processes, ionic conduction, solid phase diffusion, etc. Most of these models are sophisticated in nature and time consuming to solve [1–5]. However, some efforts have been made to simplify the complexity of the physics-based models and reduce the computation time. For example the active material concentration within the solid phase can be approximated by the second degree polynomial [6–8]. Another simplification can be obtained by using the SP model that represents each electrode as a single spherical particle and ignores the solution phase concentration and potential [9,10]. S. Santhanagopalan et al. compared the two different physics based models; the SP and the rigorous porous electrode models [11]. The parameters of each model were estimated and the statistical F-test was performed to discriminate between the models. A review of the physics-based models comprising the rigorous pseudo two dimensional (P2D), the SP and the porous electrode models with the polynomial approximation, was presented by S. Santhanagopalan et al. [12]. The second group of the models for Li-ion cell simulation is empirical or semi-empirical at best [13–15]. The majority of these models rely on the capacitor/resistor networks that are generally simple and describe the physical processes as being capacitive or resistive in nature. The original simplified circuit was adopted from Ong and Newman [16] by incorporating the double-layer capacitance into the model. M.W. Verbrugge and R.S. Conell implemented an equivalent circuit model for electrochemical and thermal characterization of a nickel metal hydride traction battery [17]. Model parameters were estimated by comparing the average cell voltage and the temperature for different charge and discharge rates. There have been some works that applied the circuit analog approach for lead acid, nickel metal hydride, Li-ion batteries and activated-carbon capacitors in adaptive manner to predict the state of charge (SOC), state of health (SOH) and power capability [18–20]. L. Gao et al. developed a model for Li-ion batteries that relies on an equivalent circuit accounting for rate and temperature dependence of the capacity, thermal dependence of the equilibrium potential and transient response [21]. Although use of manufacturers' data allows the ECA model to have good accuracy, it deviates from the experimental data at low temperature and at high discharge rates. A realistic simulation of a lithium battery pack was performed by M. Dubarry et al. [22] using an equivalent circuit approach for modeling of each single cell's performance. They showed that an accurate battery pack simulation can be achieved, if the cell-to-cell variations were taken into account. More details about the ECA model can be found in A.J. Bard and L.R. Faulkner

* Corresponding author. Tel.: +1 803 777 3270; fax: +1 803 777 0973.
E-mail address: white@cec.sc.edu (R.E. White).
[1] Electrochemical Society Student Member.
[2] Electrochemical Society Member.
[3] Electrochemical Society Fellow.

0378-7753/$ – see front matter © 2011 Elsevier B.V. All rights reserved.
doi:10.1016/j.jpowsour.2011.06.007

Nomenclature

a_{ii}	diagonal elements of the matrix A defined in Eq. (25)
AR^2	adjusted R-square
C	capacitance [F]
CI	confidence intervals of the parameters
c_e	electrolyte concentration [mol m^{-3}]
$c_{i,max}$	maximum solid phase concentration for each electrode ($i=p,n$) [mol m^{-3}]
dof	degree of freedom
$D_{s,i}$	solid phase diffusion coefficient of Li^+ or each electrode($i=p,n$) [m^2 s^{-1}]
f	the inverse of the F cumulative distribution function
F	Faraday's constant [C mol^{-1}]
H_0	null hypothesis
H_A	alternative hypothesis
I_{app}	applied current [C s^{-1}]
J	Jacobian matrix
J_i	current density at the surface of the spherical particle for each particle in electrode ($i=p,n$) [A m^{-2}]
k_i	rate constant for each electrode ($i=p,n$) [m$^{2.5}$ mol$^{-0.5}$ s^{-1}]
M	a large number
NCI	normalized confidence intervals of the parameters
n_j	number of data points for each dependent variable j
n_{nr}	number of points of independent variable
n_P	number of parameters
n_T	total number of data points
Q	columbic capacity of the cell [Ah]
PBs	prediction bounds for the fitted curves
R	cell resistance [Ω]
R^2	R-squared
R_{ct}	interfacial charge transfer resistance [Ω]
R_g	gas constant [J mol^{-1} K^{-1}]
R_i	radius particle for each electrode ($i=p,n$) [m]
r_{ij}	elements of the correlation coefficient matrix
$RMSE$	root mean squared error
s^2	approximated value for the variance
S_i	electroactive surface area for each electrode ($i=p,n$) [m^2]
SOC_i	state of charge for each electrode ($i=p,n$)
SOC_{cell}	cell state of charge
$SOC^{ch}_{0,cell}$	initial state of charge for charge
$SOC^{dch}_{0,cell}$	initial state of charge for discharge
SPB	sum of the absolute residuals between the prediction bound and the fitted model
SSE	sum of squared errors
SST	total sum of squares
t	time [s]
T	temperature [K]
U^{θ}_i	open circuit potentials for each electrode ($i=p,n$) [V]
$V(b_i)$	variance of parameter b_i
V_{cell}	cell voltage [V]
V_i	electrode volume [m^3]
V_o	open circuit potentials for the cell [V]
v	number of dependent variables
x	predictor value defined in Eq. (31)
$x_{i,avg}$	ratio of the solid average concentration to the maximum solid concentration for each electrode ($i=p,n$)
$x_{i,surf}$	ratio of the solid surface concentration to the maximum solid concentration for each electrode ($i=p,n$)
$x^0_{i,avg,ch}$	initial dimensionless average concentration for charge for each electrode ($i=p,n$)
$x^0_{i,avg,dch}$	initial dimensionless average concentration for discharge for each
y	model prediction
y^*	observed data
$\bar{y}$	mean value of the fitted responses
$\alpha_{a,i}$	cathodic transfer coefficient
$\alpha_{c,i}$	anodic transfer coefficient
β_i	true value of the parameter
η_i	overpotentials for the lithium ion intercalation reaction for each electrode ($i=p,n$) [V]
ϕ_i	potential reaction for each electrode ($i=p,n$) [V]
ε_i	active material volume fraction in the electrode ($i=p,n$)
Γ	gamma function

[23] and M.W. Verbrugge [24] books. None of the above works have compared the physics-based models to the empirical or semi-empirical models to investigate which models more accurately predict experimental data. In this paper, a comparison of the SP model [12] as a physics based approach and a simple ECA model [15] as a semi-empirical model was implemented by predicting the charge and discharge voltages at different rates for three sets of data. The nonlinear least squares method was applied to estimate the parameters of the models by using the Matlab® Curve Fitting and Global Optimization toolboxes [23]. Several statistical quantities and tests are presented in order to discriminate between the SP and ECA models.

2. Single particle model

A schematic of a lithium-ion cell represented by the SP model is depicted in Fig. 1 with an individual spherical particle representing each electrode as the current being passed through the electrode is distributed uniformly over all of the particles in the electrode. The main assumptions of the model are as follows [12]:

(1) The concentration of the electrolyte is constant and uniform for all time across the cell sandwich (cathode, separator, anode).
(2) The potential in the solution phase is constant and uniform for all time across the cell.
(3) Positive and negative electrode potentials depend on time only.
(4) There is no side reaction in the cell.

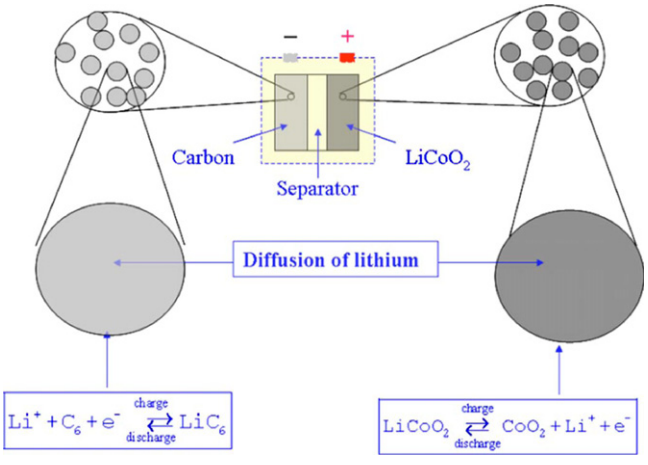

Fig. 1. A schematic of a lithium-ion cell represented by the SP model [11].

By applying a volume average technique, Fick's second law (partial differential equation), is simplified to predict the lithium ions concentration in a spherical particle. This form contains an ordinary differential equation and algebraic constraint equation (DAE) with the variables $x_{i,avg}$ and $x_{i,surf}$ $(i = p,n)$ for each of the electrodes together with their initial conditions as follows:

$$\frac{dx_{i,avg}}{dt} = \frac{-3J_i}{FR_i c_{i,\max}} \tag{1}$$

$$x_{i,surf} - x_{i,avg} = \frac{-J_i R_i}{5FD_{s,i} c_{i,\max}} \tag{2}$$

$$J_i = \frac{I_{app}}{S_i} \tag{3}$$

where $x_{i,avg}$ is the ratio of the solid average concentration to the maximum solid concentration for each electrode ($c_{i,max}$), $x_{i,surf}$ is the ratio of the solid surface concentration to the maximum solid concentration which is equal to the state of charge (SOC_i) for each electrode.

The Butler-Volmer kinetic expression is used to predict the rates of the lithium ion deintercalation and intercalation reactions for each electrode:

$$\frac{J_i}{F} = k_i (c_{i,\max} - x_{i,surf} c_{i,\max})^{0.5} (x_{i,surf} c_{i,\max})^{0.5} c_e^{0.5} \left[\exp\left(\frac{\alpha_{a,i} F}{R_g T} \eta_i\right) - \exp\left(\frac{-\alpha_{c,i} F}{R_g T} \eta_i\right) \right] \tag{4}$$

The overpotentials for the lithium ion intercalation reaction are:

$$\eta_i = \phi_i - U_i^{\theta} \tag{5}$$

The cell voltage is obtained by Eq. (6):

$$V_{cell} = \phi_p - \phi_n \tag{6}$$

Since the charge and discharge data were obtained at constant current, the model does not include the side reaction, and the cathodic and anodic transfer coefficients are the same ($\alpha_{a,i} = \alpha_{c,i} = \alpha = 0.5$), the system of differential algebraic equations (DAEs) for the SP model can be solved analytically. The analytic solution of the differential equation for the average concentration is as follows:

$$x_{i,avg} = \frac{-3J_i}{R_i F c_{i,\max}} t + x_{i,avg}^0 \tag{7}$$

Surface concentration is obtained:

$$x_{i,surf} = x_{i,avg} - \frac{J_i R_i}{5FD_{s,i} c_{i,\max}} \tag{8}$$

There are two analytic solutions for the overpotential from the Butler-Volmer equation:

$$\eta_i = \frac{R_g T}{F\alpha} \ln\left(\frac{J_i \pm (-4c_e F^2 c_{i,\max}^2 k_i^2 x^2 + 4c_e F^2 c_{i,\max}^2 k_i^2 x_{i,surf} + J_i^2)^{0.5}}{2Fc_e^{0.5} k_i (c_{i,\max} x_{i,surf})^{0.5} (c_{i,\max} - c_{i,\max} x_{i,surf})^{0.5}} \right) \tag{9}$$

where only the positive sign yields the real value (physically meaningful). Finally, the electrode potentials can be evaluated by adding the open circuit potentials to the overpotential obtained by Eq. (9):

$$\phi_i = \eta_i + U_i^{\theta}(x_{i,surf}) \tag{10}$$

The following 10 parameters of the SP model were selected to fit the data:

$$b = \left\{ D_{s,n}, D_{s,p}, S_n, S_p, k_n, k_p, x_{n,avg,ch}^0, x_{n,avg,dch}^0, x_{p,avg,ch}^0, x_{p,avg,dch}^0 \right\} \tag{11}$$

The values of the other parameters of the SP model for different cells are given in Table 1.

3. Equivalent circuit analog model

Fig. 2 shows the schematic for an equivalent circuit that represents the Li-ion cell [24].

The single equation which relates the cell current and the voltage takes the following form:

$$R\frac{dI_{app}}{dt} + \frac{1}{C}\left(1 + \frac{R}{R_{ct}}\right) I_{app} = \frac{d(V_{cell} - V_o)}{dt} + \frac{1}{R_{ct}C}(V_{cell} - V_o) \tag{12}$$

The detailed derivation is provided in [17]. Since the charge and discharge data were obtained at constant current, the differential equation for the voltage can be written as:

$$\frac{d(V_{cell} - V_o)}{dt} = \frac{1}{C}\left(1 + \frac{R}{R_{ct}}\right) I_{app} - \frac{1}{R_{ct}C}(V_{cell} - V_o) \tag{13}$$

where V_o (open circuit potential) is a function of the state of charge for the cell (SOC_{cell}).

The solution to the first order differential equation (Eq. (13)) was given in [17]:

$$V_{cell} = V_o + IR + \frac{Q}{C}\exp\left(\frac{-t}{R_{ct}C}\right) + I_{app}R_{ct}\left(1 - \exp\left(\frac{-t}{R_{ct}C}\right)\right) \tag{14}$$

The SOC_{cell} is changed with time as follows:

$$SOC_{cell} = SOC_{0,cell} + \frac{I_{app}}{3600Q} t \tag{15}$$

where $SOC_{0,cell}$ is the initial SOC for the cell. Note that the current is positive while charging the cell and negative when the cell is discharged. The open circuit potential, V_o, for the cell is calculated as the difference of the open circuit potentials for the electrodes:

$$V_o = U_p^{\theta}\left(SOC_p\right) - U_n^{\theta}(SOC_n) \tag{16}$$

In order to evaluate the open circuit potentials for the electrodes, the state of charge of the cell must be correlated to the SOC of each electrode. The values of electrode SOCs are known at the fully charged state, i.e. $SOC_{cell} = 1.0$, and the fully discharged state, i.e. $SOC_{cell} = 0.0$. Thus, the SOC for each electrode at a particular cell SOC can be determined by using a linear interpolation.

The following 6 parameters of the ECA model were considered to be estimated to fit the data:

$$b = \left\{ C, Q, R, R_{ct}, SOC_{0,cell}^{ch}, SOC_{0,cell}^{dch} \right\}$$

where $SOC_{0,cell}^{ch}$, $SOC_{0,cell}^{dch}$ are the initial cell SOC for charge and discharge, respectively.

4. Parameter estimation

Matlab® Curve Fitting and Global Optimization toolboxes [25] were used to estimate the parameters of the SP and the ECA models using the nonlinear least squares method. To compare the models statistically, the following are presented for each model:

- Sum of squares due to error (*SSE*)
- *R*-square (R^2), adjusted *R*-square (AR^2), root mean squared error (*RMSE*), confidence intervals of the Parameters (*CI*)
- Normalized confidence intervals of the parameters (*NCI*)
- Prediction bounds for the fitted curves (*PBs*)
- Sum of the absolute residuals between the prediction bound and the fitted model (*SPB*)

Also the statistical *t*-test was performed to show the significance of the parameters of the models and in order to test the adequacy of the models, the *F*-test and the χ^2-test are presented.

Table 1
SP model constant parameters in parameter estimation for different cells.

Parameters	USG		Quallion		P2D	
	Value	Unit	Value	Unit	Value	Unit
$c_{p,max}$	51,555	mol m^{-3}	50,991	mol m^{-3}	51,555	mol m^{-3}
$c_{n,max}$	30,555	mol m^{-3}	30,555	mol m^{-3}	30,555	mol m^{-3}
c_e	1000	mol m^{-3}	1000	mol m^{-3}	1000	mol m^{-3}
R_p	1e−5	m	5e−6	m	8.5e−6	m
R_n	2.5e−5	m	1.25e−5	m	12.5e−5	m
$\alpha_{a,i}$	0.5	–	0.5	–	0.5	–
$\alpha_{c,i}$	0.5	–	0.5	–	0.5	–
T	298.15	K	298.15	K	298.15	K
R	8.3143	J mol^{-1} K^{-1}	8.3143	J mol^{-1} K^{-1}	8.3143	J mol^{-1} K^{-1}
F	96,487	C mol^{-1}	96,487	C mol^{-1}	96,487	C mol^{-1}

5. Nonlinear least squares

Because the SP and the ECA models are nonlinear in their parameters, the nonlinear least squares method was applied to minimize the *SSE* between the experiments and the model given by [26]:

$$SSE = \sum_{j=1}^{v}\sum_{i=1}^{n_j}(y_{ij}^{*} - y_{ij})^2 \quad (17)$$

where v and n_j are the number of dependent variables and the number of data points for each variable, respectively; and y_{ij}^{*}, y_{ij} are the observed response and the fitted response values, respectively. The objective function, *SSE*, is minimized using the trust region method (Curve Fitting toolbox) and the genetic algorithm (Global Optimization toolbox) in the following procedure:

1. Initial guess, lower and upper bounds for the parameters are selected.

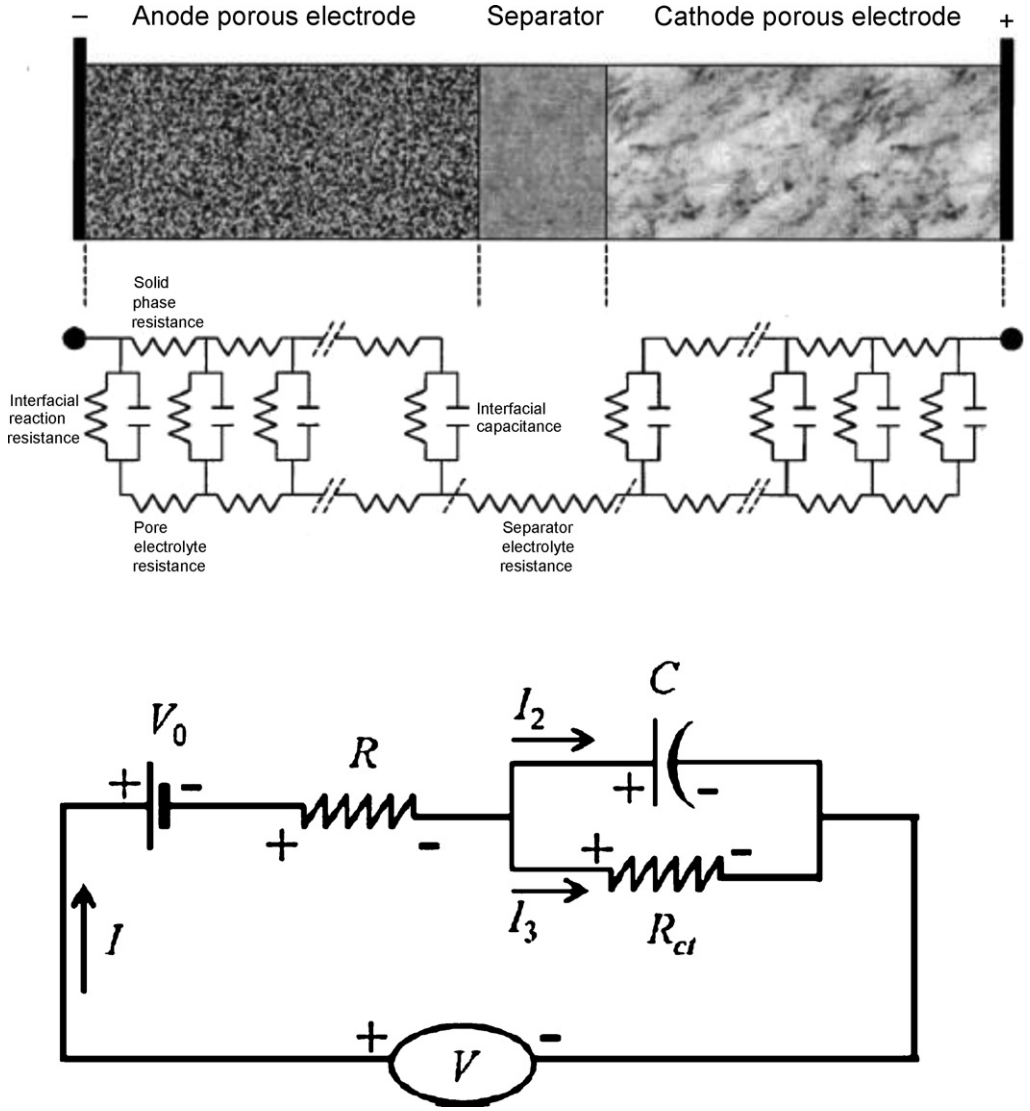

Fig. 2. Equivalent circuit for correlating the lithium-ion cell behavior [24].

2. The trust region method tries to minimize the objective function using the initial guess. Note that the Levenberg-Marquardt method does not handle the bound constraints.
3. The resulting point from Step 2 is considered as one of the children of the initial population in the genetic algorithm while the other children are generated randomly in the feasible domain for the parameters. Afterward, the genetic tried to find the parameters with less *SSE*.
4. If the objective function is improved in Step 3 by a defined tolerance ($\varepsilon_{imp} = 10^{-6}$), the optimal parameters obtained in Step 3 are picked as the initial guess for Step 2; otherwise terminate the minimization algorithm and print the results.

R^2 is expressed as [27]:

$$R^2 = 1 - \frac{SSE}{SST} \tag{18}$$

where *SST*, the total sum of squares, is defined as [27]:

$$SST = \sum_{i=1}^{n_T} \left(y_i^* - \bar{y}\right)^2 \tag{19}$$

where n_T and $\bar{y}$ are total number of data points and the mean value of the fitted responses, respectively. Note that because all the dependent variables are cell voltages, we define a unique R^2 for all the curves. Since the number of parameters for the SP and the ECA are different, the AR^2 and the *RMSE* are also presented in this work as follows [27]:

$$AR^2 = 1 - \frac{(n_T - 1)SSE}{(dof - 1)SST} \tag{20}$$

$$RMSE = \sqrt{\frac{SSE}{dof}} \tag{21}$$

$$dof = n_T - n_P \tag{22}$$

where *dof* and n_P are the degree of freedom and the number of parameters, respectively.

The 95% confidence interval for the parameter b_i is constructed as [26]:

$$CI_i = \pm t_{(1-0.05/2)} s\sqrt{a_{ii}} \tag{23}$$

where $t_{(1-0.05/2)}$ is a value of Student's *t*-distribution with *dof* degrees of freedom and 95% confidence, and s^2, approximated value for the variance, is given by [26]:

$$s^2 = \frac{SSE}{dof} \tag{24}$$

a_{ii} in Eq. (23) are the diagonal elements of the following matrix [26]:

$$A = \left(\sum_{j=1}^{v} J_j^T J_j\right)^{-1} \tag{25}$$

where *J* is the Jacobian matrix defined at each point as follows:

$$J = \frac{\partial SSE}{\partial b_i} \tag{26}$$

The elements of the correlation coefficient matrix are calculated by Eq. (27) to show how the parameters of the models are correlated [26]:

$$r_{ij} = \frac{Cov(b_i, b_j)}{\sqrt{V(b_i)V(b_j)}} \tag{27}$$

where $Cov(b_i, b_j)$, $V(b_i)$ are the covariance of b_i and b_j and the variance of b_i is obtained as follows:

$$\begin{aligned} Cov(b_i, b_j) &= s^2 a_{ij} \\ V(b_i) &= s^2 a_{ii} \end{aligned} \tag{28}$$

By substituting Eq. (28) in Eq. (27), the following is obtained:

$$r_{ij} = \frac{a_{ij}}{\sqrt{a_{ii}a_{jj}}} \tag{29}$$

where a_{ij} is the (i,j) element of the matrix *A* defined in Eq. (25). The higher the correlation between two parameters, the closer the absolute value of r_{ij} is to 1.0.

We defined the normalized parameter confidence interval (NCI) in this paper in order to compare the confidence interval for different parameters and also for different models:

$$NCI_i = \frac{\pm t_{(1-0.05/2)} s\sqrt{a_{ii}}}{b_i} \tag{30}$$

The prediction upper and lower bounds (PB^{UL}) for the fitted curve and for all predictor values (x) are given by [27]:

$$PB^{UL} = y \pm fs\sqrt{xa_{ii}x^T} \tag{31}$$

where *f* is the inverse of the *F* cumulative distribution function. The *PB*s together with the fitted curves for the SP and the ECA models are presented. However, the sum of the absolute residuals between the lower bounds (lower or upper bounds results in no difference) and the fitted model is also calculated to compare the bounds of the models quantitatively:

$$SPB = \sum_{j=1}^{v}\sum_{i=1}^{n_j} \left(PB^L - y_{ij}\right) \tag{32}$$

6. *t*-test

A significant test (*t*-test) presented in [26] is to test the null hypothesis that any one of the parameters might be equal to zero. The null hypothesis can be stated as [26]:

$$H_0 : \beta_i = 0$$

and the alternative hypothesis as

$$H_A : \beta_i \neq 0$$

This is true when the parameter appears in the model as the parameter vanishes if the value is set to zero such as polynomial coefficients. Thus, when the test verifies the null hypothesis, the parameter can be removed from the model. However, this is not the case when the parameter is the root of a denominator or the root of a natural logarithm, etc. For the former, β_i needs to be a large number while for the latter β_i is one. For example, consider the following model with two parameters (b_1, b_2):

$$y = \frac{x}{b_1} + \ln(b_2)$$

The null hypothesis can be stated as

$$H_0 : \beta_1 = M, \quad \beta_2 = 1$$

and the alternative hypothesis as

$$H_A : \beta_1 \neq M, \quad \beta_2 \neq 1$$

where *M* is a large number. As a result, when the null hypothesis is accepted, the parameter can be eliminated in the model.

Table 2
Optimization results for fitting the USG and P2D data using the SP and the ECA models.

USG using the SP model		USG using the ECA model		P2D using the SP model		P2D using the ECA model	
Initial guess/method	*SSE*	Initial guess/method	*SSE*	Initial guess/method	*SSE*	Initial guess/method	*SSE*
Initial guess	1060570	Initial guess	295.109	Initial guess	157617	Initial guess	485.126
Trust region	959662	Trust region	2.6536	Trust region	155556	Trust region	0.70651
Genetic	0.6043	Genetic	2.6536	Genetic	0.03437	Genetic	0.61433
Trust region	0.4963			Trust region	0.01351	Trust region	0.61368
Genetic	0.4963			Genetic	0.01351	Genetic	0.61368

The t value is calculated for each parameter using the following equation:

$$t = \frac{b_i - \beta_i}{s\sqrt{a_{ii}}} \tag{33}$$

If this value lies within the region of acceptance given by the t distribution at the required confidence interval level, then the null hypotheses is accepted.

7. *F*-test

In order to test the adequacy of the fit of the SP and the ECA models, the *F*-test was performed [26]. The total sum of residuals is the sum of the error due to the lack of fit and the experimental error. The variances of these errors are obtained using the following equations:

$$\begin{aligned} s_1^2 &= \frac{\sum_{i=1}^{n_{nr}} (y_i - \bar{y}^*)^2}{dof_1} \\ s_2^2 &= \frac{\sum_{i=1}^{n_{nr}} (y^* - \bar{y}^*)^2}{dof_2} \\ dof_1 &= n_{nr} - n_p \\ dof_2 &= n_T - n_{nr} \end{aligned} \tag{34}$$

where $\bar{y}^*$ is the mean value of each group of repeated experiments, n_{nr} is the number of points of independent variable (the total non repeated points), and n_T is the total number of points. The ratio of the variances, s_1^2/s_2^2, has an F distribution with dof_1 and dof_2 degrees of freedom. For a good fit, the following inequality must be true:

$$\frac{s_1^2}{s_2^2} < F_{1-\alpha}(dof_1, dof_2) \tag{35}$$

$F_{1-\alpha}(dof_1, dof_2)$ value can be calculated by solving the following equation:

$$\begin{aligned} &\int_0^{F_{1-\alpha}(dof_1, dof_2)} f(t, dof_1, dof_2)dt = 1 - \alpha \\ &f(t, dof_1, dof_2) = \frac{\Gamma((dof_1 + dof_2)/2)}{\Gamma(dof_1/2)\Gamma(dof_2/2)} \left(\frac{dof_1}{dof_2}\right)^{\frac{dof_1}{2}} \frac{t^{(dof_1-2)/2}}{[1 + (dof_1/dof_2)t]^{(dof_1+dof_2)/2}} \end{aligned} \tag{36}$$

where Γ is the gamma function.

8. Chi-squared (χ^2) test

In order to show the goodness of the fit, the chi-squared (χ^2) statistical test is also accomplished [28]. The quantity known as chi-squared (χ^2) is calculated as follows:

$$\begin{aligned} \chi^2 &= \sum_{i=1}^{n_{nr}} \frac{(y_i - \bar{y}^*)}{va^*} \\ va^* &= \sum_{j=1}^{n^*} (y^* - \bar{y}^*)^2 \end{aligned} \tag{37}$$

This quantity has a χ^2 distribution with dof_1 degrees of freedom and to have a good fit, the following muse be satisfied:

$$\chi^2 < \chi^2_{dof_1, 1-\alpha} \tag{38}$$

where $\chi^2_{dof_1, 1-\alpha}$ is obtained by solving the following equation:

$$\begin{aligned} &\int_{\chi^2_{dof_1, 1-\alpha}}^{\infty} f(\chi^2)d\chi^2 = 1 - \alpha \\ &f(\chi^2) = \frac{e^{-\chi^2/2}(\chi^2)^{(dof_1/2)-1}}{2^{dof_1/2}\Gamma\left(\frac{dof_1}{2}\right)} \end{aligned} \tag{39}$$

Table 3
Statistical results for the USG data fitting using the SP model.

Parameter	10 Parameter model			8 Parameter model				
	Value	*t* value	Is parameter significantly affecting the fitting?	Value	*CI*	*NCI*	*t* value	Is parameter significantly affecting the fitting?
$D_{s,n}$ ($m^2\ s^{-1}$)	1.3863e−14	−27691	Yes	1.3862e−14	±4.0258e−15	±0.29042	−48678	Yes
$D_{s,p}$ ($m^2\ s^{-1}$)	9.9984e−11	−1.9e−6	No	–	–	–	–	–
S_n (m^2)	0.14477	–	–	0.14489	±0.021376	±0.14753	–	–
S_p (m^2)	0.18868	–	–	0.18867	±0.0018607	±0.0098621	–	–
k_n ($m^{2.5}\ mol^{-.5}\ s^{-1}$)	9.9991e−6	−2.3e−9	No	–	–	–	–	–
k_p ($m^{2.5}\ mol^{-.5}\ s^{-1}$)	4.7568e−12	−2.6e7	Yes	4.7585e−12	±1.9004e−13	±0.039937	−1.03e8	Yes
$x^0_{n,avg,ch}$	0.11119	7.1139	Yes	0.11136	±0.015185	±0.13636	14.244	Yes
$x^0_{n,avg,dch}$	0.83869	29.497	Yes	0.83814	±0.053812	±0.064204	30.491	Yes
$x^0_{p,avg,ch}$	0.99534	6794.1	Yes	0.99534	±0.00014166	±0.00014232	13757	Yes
$x^0_{p,avg,dch}$	0.5313	171.59	Yes	0.53128	±0.004497	±0.0084645	231.11	Yes

9. Results and discussion

9.1. USG Gen 1.0 experimental data

The experimental data consists of the cell voltage, current and the temperature for several charge/discharge cycles of the lithium-ion pouch cell. The rated capacity of the cell is 341 mA h. The active materials of the positive and negative electrodes are lithium cobalt oxide ($LiCoO_2$) and mesocarbon microbead (MCMB) 2528, respectively. The three first charge curves at 0.2 *C*-rate and three discharge curves at different rates, 0.5, 0.686, and 1.029 *C*-rates were selected to estimate the parameters of the SP and the ECA models. The anode and cathode open-circuit potentials as functions of the SOCs are expressed as [5]:

$$U_n(SOC_n) = .7222 + .1387SOC_n + .029SOC_n^{1/2} - \frac{.0172}{SOC_n} + \frac{.0019}{SOC_n^{1.5}} + .2808e^{(0.9-15SOC_n)} - .7984e^{(0.4465SOC_n-0.4108)}$$

$$U_p(SOC_p) = \frac{-4.656 + 88.669SOC_p^2 - 401.119SOC_p^4 + 342.909SOC_p^6 - 462.471SOC_p^8 + 433.434SOC_p^{10}}{-1 + 18.933SOC_p^2 - 79.532SOC_p^4 + 37.311SOC_p^6 - 73.083SOC_p^8 + 95.96SOC_p^{10}}$$

It is assumed that the anode and cathode SOCs vary linearly with the cell SOC as already mentioned. Fig. 1 in [29] was used to obtain the following linear functions:

$$\begin{cases} SOC_a = 0.79SOC_{cell} + 0.01 \\ SOC_c = 0.97 - 0.51SOC_{cell} \end{cases}$$

9.1.1. SP model

The SP model includes the following 10 parameters:

$$b = \left\{D_{s,n}, D_{s,p}, S_n, S_p, k_n, k_p, x^0_{n,avg,ch}, x^0_{n,avg,dch}, x^0_{p,avg,ch}, x^0_{p,avg,dch}\right\}$$

The diffusion term in the model can be removed when the diffusion coefficient becomes large. As a result, β_i in the *t* value equation is set to the upper bound ($10^{-5}\,m^2\,s^{-1}$) used in the optimization. The active surface area (S_i) is also required to be a large number for elimination in the model. However, the upper bound for this parameter is limited to the theoretical value that cannot be considered as the value for β_i. Thus, the *t* value is not defined for the S_i. In order to eliminate the kinetic parameters (k_i) in the model, the expression in the natural logarithm of the overpotential equation is needed to be one. This occurred when the k_i limit to the infinity, which means there is no reaction resistance for intercalation or deintercalation of Li^+ ions in the electrodes. Thus, β_i needs to be a large number. The upper bound ($10^{-10}\,m^{2.5}\,mol^{-0.5}\,s^{-1}$) used in the optimization for the k_i is considered as β_i. The β_i values for the initial SOCs are zero as these parameters are linear in the model. Table 2 presents the objective function improvement by using the optimization algorithm. The genetic algorithm greatly improved the objective function after the trust region method as shown in Table 2. The parameters' values and the corresponding *t* values are given in Table 3. The table indicates that the cathode diffusion coefficient and the anode rate constant do not affect the fitting significantly. Thus, the regression was repeated for the model with 8 remaining parameters. In the new model, since there is no diffusion resistance for the positive electrode, the surface concentration is the same as the average concentration and the negative electrode potential is equal to the open circuit potential because there is no reaction resistance:

$$x_{p,surf} = x_{p,avg}$$
$$\phi_n = U_n^{\theta}(x_{n,surf})$$

The initial state of charge of the positive electrode returned from the parameter estimation routine is larger than expected ($0.99 \le x^0_{p,avg,ch} \le 1.0$). The large value is likely due to the fact that the SP model does not take into account the potential drop in the electrolyte.

Table 3 consists of the parameters' values, confidence intervals, normalized confidence intervals, and *t* values. The same *SSE* for the 10 parameter SP model was obtained. The fitted SP model and the prediction bounds for different charge and discharge rates are shown in Fig. 3a and b, respectively. In order to check the validity of the values of the active surface areas obtained by the parameter estimation, the active material volume fractions in the electrodes are calculated as follows:

$$\varepsilon_i = \frac{R_i S_i}{3V_i}$$

The projected areas for the positive and negative electrodes are 0.0213 and 0.0226 m^2, respectively. Since the thicknesses are 53 and 72 μm for the positive and negative electrodes respectively, the active material volume fractions were calculated as 0.558 for the positive and 0.743 for the negative.

9.1.2. ECA model

The following 6 parameters were used in the ECA model to fit the data:

$$\left\{C, Q, R, R_{ct}, SOC^{ch}_{0,cell}, SOC^{dch}_{0,cell}\right\}$$

The value of β_i for capacitance *C* is a large number (e.g. upper bound of the optimization (10,000 F)) because as capacitance *C* limits to the infinity, the corresponding term in the model can be eliminated. For other parameters, β_i is zero. The optimization results are shown in Table 2. In this case, the genetic did not improve the *SSE* after the trust region method. Table 4 presents the least squares results including the parameters' values and the *t* values. The *t* value for resistance *R* lies within the region of acceptance of the null hypothesis given by the *t* distribution at the 95% confidence interval. This means that resistance *R* can be removed in the model and as a result we need to repeat the least squares algorithm for the model with remaining 5 parameters. The results are given in Table 4. It can be seen that the *t* value of the interfacial charge transfer resistance, R_{ct}, is enhanced more with respect to the other parameters when the resistance *R* is eliminated. Fig. 4a and b illustrates the fitted ECA model and the prediction bounds for the charge and discharge rates, respectively.

9.1.3. Comparison

Table 5 presents the statistical quantities resulting obtained by fitting the USG data using the SP and the ECA models. Based on the results in the table, it is obvious that the SP model predicts the USG data much superior than the ECA model.

9.2. Quallion Gen 2.0 experimental data

One charge curve and one discharge curve both at 0.393 *C*-rate (0.9825 A) were selected among several charge/discharge cycles' experimental data obtained from the natural graphite (Mag-10)/Li half-cell, $LiNi_{0.8}Co_{0.15}Al_{0.05}O_2$/Li half-cell. The rated capacity of the cell is 2.5 Ah. The open circuit potentials versus the SOC of the active material in the positive and negative electrodes have been reported

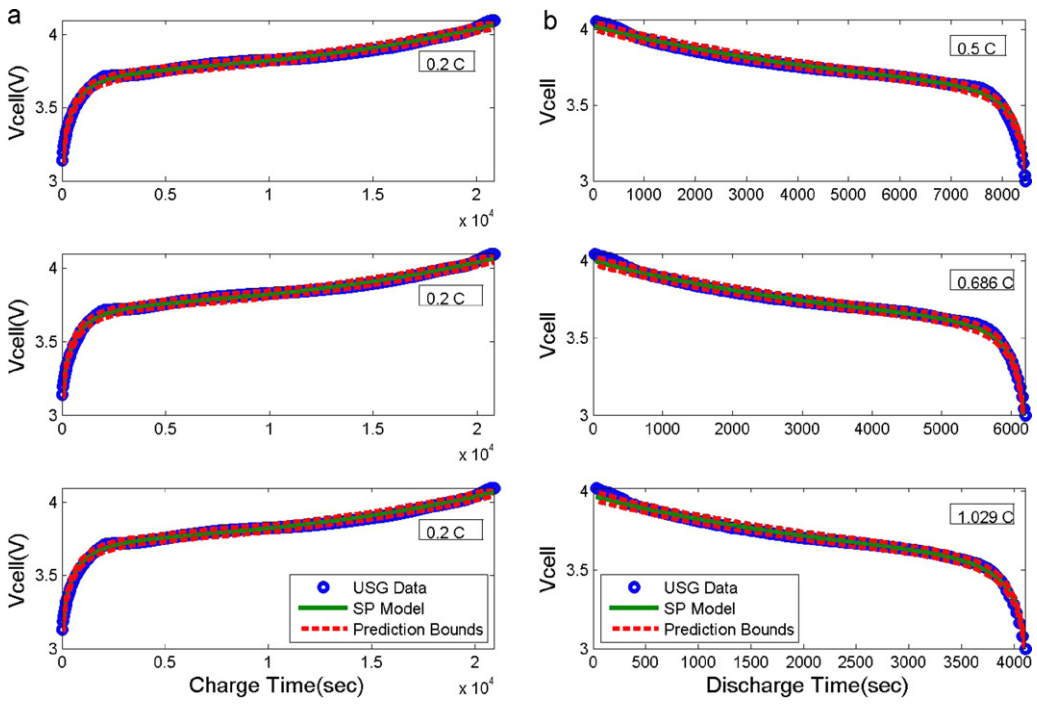

Fig. 3. The fitted SP model with 8 parameters and the prediction bounds for USG data (a) charge and (b) discharge.

Table 4
Statistical results for the USG data fitting using the ECA model.

Parameter	6 Parameter model			5 Parameter model				
	Value	*t* value	Is parameter significantly affecting the fitting?	Value	*CI*	*NCI*	*t* value	Is parameter significantly affecting the fitting?
C (F)	1795.6	−16.57	Yes	1793.8	±514.3	±0.2869	−31.278	Yes
Q (Ah)	0.49344	364.38	Yes	0.49344	±0.0026525	±0.0053757	364.6	Yes
R (Ω)	1.170e−8	3.727e−7	No	–	–	–	–	–
R_{ct} (Ω)	0.27783	8.5218	Yes	0.2778	±0.012425	±0.044728	43.819	Yes
$SOC_{cell}{}^{ch}$	0.037499	43.383	Yes	0.037503	±0.0016396	±0.043728	44.821	Yes
$SOC_{cell}{}^{dch}$	0.82258	370.92	Yes	0.82258	±0.0043451	±0.0052822	371.05	Yes

in [30]. The following linear functions for the anode and the cathode SOCs variations with the cell SOC obtained based on Fig. 3 in [30]:

$$\begin{cases} SOC_a = 0.7388SOC_{cell} + 0.0252 \\ SOC_c = -0.62 + 0.96SOC_{cell} \end{cases}$$

9.2.1. SP model

Table 6 lists the values of the parameters and the *t* values obtained by fitting the Quallion data using the SP model with 10 parameters. The table indicates that the diffusion coefficients for both electrodes and all initial SOCs do not influence the fitting significantly. However, the correlation coefficient matrix for the parameters states that the SOCs for each electrode are correlated with the electrode diffusion coefficient as shown in Table 7. As a result, we repeated the regression with 8 parameter model that excludes the diffusion coefficients because their *t* values are less than the others. Thus, the Li ion surface concentrations are assumed to be equal to the average concentration for both electrodes. The statistical results are presented in Table 6. Fig. 5a and b shows the fitted SP model and the prediction bounds for charge and discharge rates, respectively.

Table 5
Comparison of the SP model with the ECA model for fitting different data.

Data	Model	# of the parameters	*dof*	*SSE*	R^2	AR^2	*RMSE*	*SPB*	$\frac{s_1^2}{s_2^2}$	χ^2 value
USG	SP	8	2704	0.49625	0.99214	0.99212	0.013547	72.147	–	–
	ECA	5	2707	2.6536	0.95798	0.95792	0.031309	166.65	–	–
Quallion	SP	8	100	0.01414	0.99911	0.99905	0.011891	2.6431	–	–
	ECA	5	103	0.24647	0.98456	0.98396	0.048917	10.713	–	–
	ECA[a]	8	100	0.039934	0.9975	0.99732	0.019983	4.4325		
P2D	SP	9	231	0.01351	0.99864	0.99859	0.007647	3.6814	1.6582	344.05
	ECA	5	235	0.61368	0.93808	0.93702	0.051102	24.404	74.041	14210

[a] ECA with quadratic R_{ct}.

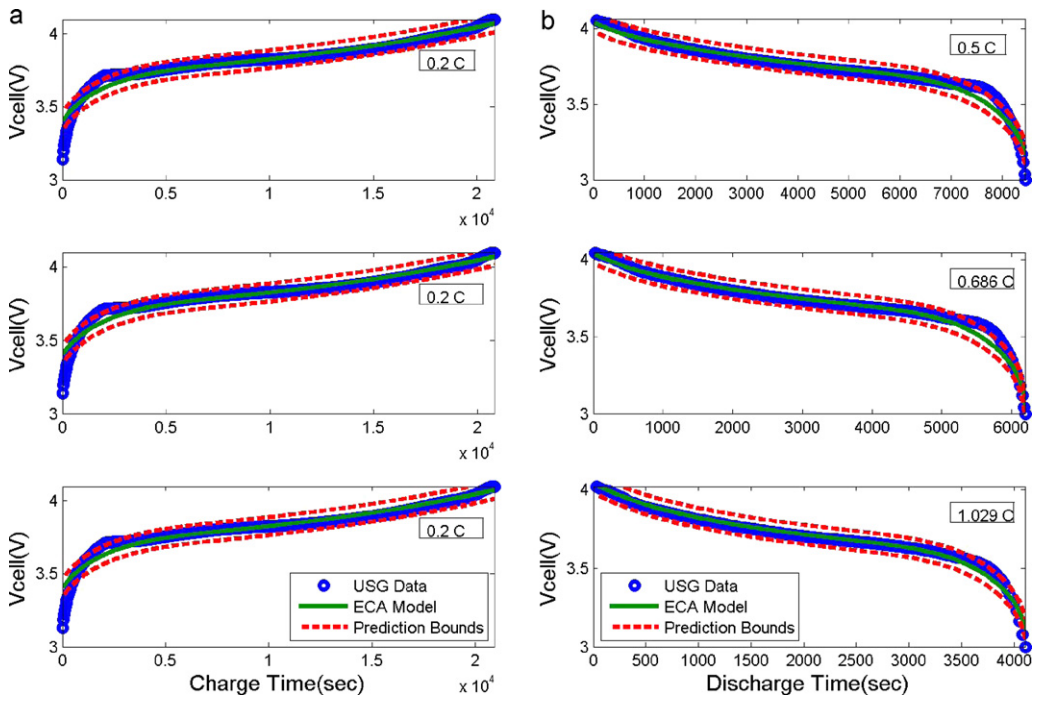

Fig. 4. The fitted ECA model with 5 parameters and the prediction bounds for the USG data (a) charge and (b) discharge.

Table 6
Statistical results for the Quallion data fitting using the SP model.

Parameter	10 Parameter model			8 Parameter model				
	Value	*t* value	Is parameter significantly affecting the fitting?	Value	*CI*	*NCI*	*t* value	Is parameter significantly affecting the fitting?
$D_{s,n}$ ($m^2\ s^{-1}$)	3.7077e−11	−8.1e−9	No	–	–	–	–	–
$D_{s,p}$ ($m^2\ s^{-1}$)	9.999e−11	−2e−15	No	–	–	–	–	–
S_n (m^2)	0.77424	–	–	0.77423	±0.0047632	±0.0061521	–	–
S_p (m^2)	2.2962	–	–	2.2962	±0.034462	±0.015008	–	–
k_n ($m^{2.5}\ mol^{-.5}\ s^{-1}$)	1.3572e−10	−1.8e5	Yes	1.3567e−10	±1.3742e−10	±1.0129	−1.4e5	Yes
k_p ($m^{2.5}\ mol^{-.5}\ s^{-1}$)	1.0191e−12	−7.2e7	Yes	1.0192e−12	±2.7152e−13	±0.2664	−7.3e7	Yes
$x^0_{n,avg,ch}$	0.045253	7.2e−6	No	0.045282	±0.0041508	±0.091666	21.165	Yes
$x^0_{n,avg,dch}$	0.92108	1.5e−4	No	0.92105	±0.0056974	±0.0061857	320.39	Yes
$x^0_{p,avg,ch}$	0.90801	1.7e−5	No	0.908	±0.010002	±0.011015	179.91	Yes
$x^0_{p,avg,dch}$	0.42561	8e−6	No	0.42561	±0.0090567	±0.021279	93.015	Yes

Table 7
Correlation coefficient matrix for the Quallion data fitting using the SP model with 10 parameters.

Parameters	$D_{s,n}$	$D_{s,p}$	S_n	S_p	k_n	k_p	x_1 [a]	x_2 [b]	x_3 [c]	x_4 [d]
$D_{s,n}$	1	0.32	−5.6e−7	2.4e−7	−1.6e−7	1.42e−7	1	−1	−0.32	0.32
$D_{s,p}$	0.32	1	−1.3e−7	3.8e−8	−1.9e−8	4.2e−8	0.32	−0.32	−1	1
S_n	−5.6e−7	−1.3e−7	1	−0.4	0.22	−0.26	−4.4e−7	8.7e−8	1.6e−7	−1.6e−7
S_p	2.4e−7	3.3e−8	−0.4	1	−0.61	0.06	3.9e−8	−4.5e−8	−6.4e−8	5.2e−8
k_n	−1.6e−7	−1.9e−8	0.22	−0.61	1	−0.29	4.1e−8	3.1e−8	3.1e−8	−1.5e−8
k_p	1.4e−7	4.2e−8	−0.26	0.06	−0.29	1	1.3e−7	−1.2e−8	−1.3e−7	1.2e−7
x_1 [a]	1	0.32	−4.4e−7	3.9e−8	4.1e−8	1.3e−7	1	−1	−0.32	0.32
x_2 [b]	−1	−0.32	8.7e−8	−4.5e−8	3.1e−8	−1.2e−8	−1	1	0.32	−0.32
x_3 [c]	−0.32	−1	1.6e−7	−6.4e−8	3.1e−8	−1.3e−7	−0.32	0.32	1	−1
x_4 [d]	0.32	1	−1.6e−7	5.2e−8	−1.5e−8	1.2e−7	0.32	−0.32	−1	1

[a] $x_1 = x^0_{n,avg,ch}$.
[b] $x_2 = x^0_{n,avg,dch}$.
[c] $x_3 = x^0_{p,avg,ch}$.
[d] $x_4 = x^0_{p,avg,dch}$.

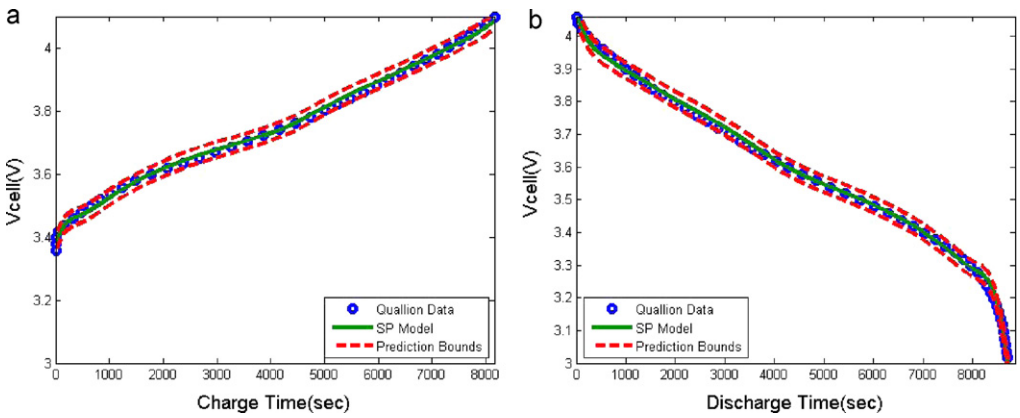

Fig. 5. The fitted SP model with 8 parameters and the prediction bounds for the Quallion data (a) 0.393 *C*-rate charge and (b) 0.393 *C*-rate discharge.

Table 8
Statistical results for the Quallion data fitting using the ECA model.

Parameter	6 Parameter model			5 Parameter model				
	Value	*t* value	Is parameter significantly affecting the fitting?	Value	*CI*	*NCI*	*t* value	Is parameter significantly affecting the fitting?
C (F)	128.43	−53.725	Yes	87.275	±155.58	±1.7826	−126.36	Yes
Q (Ah)	2.833	65.794	Yes	2.8369	±0.078185	±0.02756	71.961	Yes
R (Ω)	0.031992	0.92098	No	–	–	–	–	–
R_{ct} (Ω)	0.030438	0.92165	No	0.061486	±0.014926	±0.24276	8.1696	Yes
$SOC_{cell}{}^{ch}$	0.081913	5.5514	Yes	0.084271	±0.026832	±0.3184	6.2288	Yes
$SOC_{cell}{}^{dch}$	0.84882	65.796	Yes	0.84765	±0.023361	±0.027559	71.963	Yes

9.2.2. ECA model

The parameters' values with corresponding *t* values obtained by fitting the Quallion data using the ECA model with 6 parameters are listed in Table 8. Although the *t* values for both resistances *R* and R_{ct} verify the null hypothesis, the correlation coefficient matrix shows a correlation between them. Thus, the model that excludes only resistance *R* is used to fit the data. The parameters values together with confidence interval and *t* values are given in Table 8. The fitted ECA model and the prediction bounds for the charge and discharge rates are depicted in Fig. 6a and b, respectively.

9.2.3. Comparison

The comparison between the SP and the ECA models are given in Table 5 that indicates that the SP model goodness of the fit surpasses the fit for the ECA model.

9.3. Pseudo two dimensional (P2D) model data

In order to accomplish the *F* and χ^2 statistical tests for the SP and the ECA models, a zero mean Gaussian noise with the specified standard deviation (e.g. 0.01) is added to the data obtained by running the rigorous P2D model in COMSOL 3.5a environment [31] under the four different charge/discharge rates, 0.1, 0.25, 0.5 and 1.0 *C*-rate. Three replicates were generated at each independent variable point. The same chemistry as the USG cell but with different dimensions was used and the cell rated capacity was 1.656 Ah.

9.3.1. SP model

Table 9 lists the values of the parameters and the *t* values obtained by fitting the P2D data using the SP model with 10 parameters. The table indicates that the diffusion coefficients for the positive electrodes do not affect the fitting significantly. Thus, the

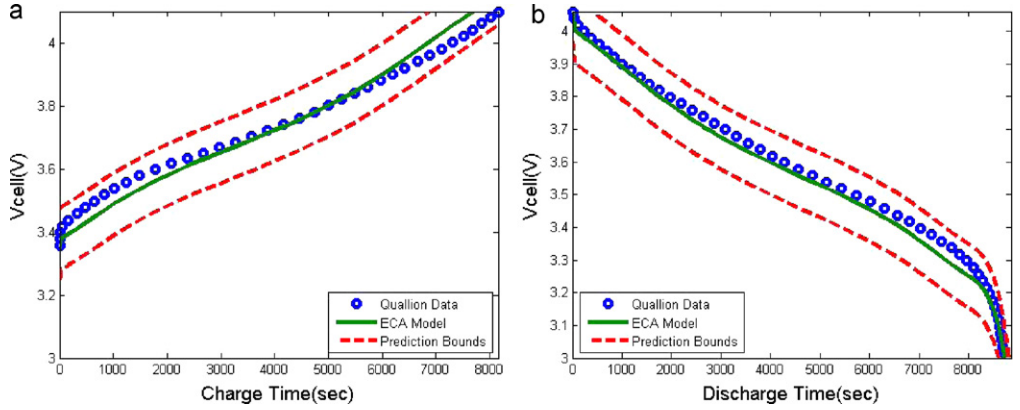

Fig. 6. The fitted ECA model with 5 parameters and the prediction bounds for the Quallion data (a) 0.393 *C*-rate charge and (b) 0.393 *C*-rate discharge.

Table 9
Statistical results for the P2D data fitting using the SP model.

Parameter	10 Parameter model			9 Parameter model				
	Value	*t* value	Is parameter significantly affecting the fitting?	Value	*CI*	*NCI*	*t* value	Is parameter significantly affecting the fitting?
$D_{s,n}$ ($m^2\ s^{-1}$)	5.5529e−14	−2.9e5	Yes	5.5529e−14 (5.5e−14)[a]	±6.767e−16	±0.012186	−2.9e5	Yes
$D_{s,p}$ ($m^2\ s^{-1}$)	1e−10	−2e−16	No	−(1e−11)[a]	–	–	–	–
S_n (m^2)	0.68396	–	–	0.68395 (0.78794)[a]	±0.010436	±0.015258	–	–
S_p (m^2)	1.131	–	–	1.131 (1.1442)[a]	±0.010912	±0.0096481	–	–
k_n ($m^{2.5}\ mol^{-.5}\ s^{-1}$)	1.1067e−11	−1.4e7	Yes	1.1068e−11 (1.764e−11)[a]	±1.3737e−12	±0.12412	−1.4e7	Yes
k_p ($m^{2.5}\ mol^{-.5}\ s^{-1}$)	4.2239e−11	−9.24e5	Yes	4.219e−11 (6.667e−11)[a]	±1.7664e−11	±0.41867	−1.1e6	Yes
$x^0_{n,avg,ch}$	0.070546	11.614	Yes	0.070486 (0.05)[a]	±0.011504	±0.1632	11.901	Yes
$x^0_{n,avg,dch}$	0.82842	124.79	Yes	0.82845 (0.756)[a]	±0.012442	±0.015018	131.04	Yes
$x^0_{p,avg,ch}$	0.97272	528.63	Yes	0.9727 (0.95)[a]	±0.0033922	±0.0034874	564.39	Yes
$x^0_{p,avg,dch}$	0.46384	536.91	Yes	0.46384 (0.465)[a]	±0.0011285	±0.0024329	808.09	Yes

[a] P2D model parameters.

regression was repeated with 9 parameter model excluding the positive electrode's diffusion coefficient. Table 9 and Fig. 7a and b present the results (only the data for 1.0 *C*-rate (1.656 A) charge and discharge) obtained by fitting the P2D data using the SP model with 9 parameters. The genetic algorithm, also, in this case improved the objective function significantly after the trust region method as shown in Table 2. The input parameters of the P2D model are also given in Table 9 that indicates the parameters of the P2D and the SP models are in the same order of magnitude.

9.3.2. ECA model

The parameter estimation results obtained by fitting the P2D data using the ECA model with 6 parameters are listed in Table 10. Although the *t* values for both resistances *R* and R_{ct} verify the null hypothesis, the correlation coefficient matrix shows a correlation between them. Based on the model equations, we decided to exclude resistance *R* since the resistance R_{ct} is in the two terms of the model while resistance *R* is only in one term of the equation. The remaining 5 parameters' values together with their confidence intervals and *t* values are given in Table 10. The improvement of the objective function is presented in Table 2. The fitted ECA model and the prediction bounds for only 1.0 *C*-rate charge and discharge are depicted in Fig. 8a and b.

9.4. Comparison

Table 5 compared the SP and the ECA models for fitting the P2D data. At the 95% confidence interval, the values for $F_{95\%}(dof_1, dof_2)$ and $\chi^2_{dof_1,95\%}$ for the SP model are calculated as 1.2009 and 267.46 respectively using the Matlab® Statistics Toolbox and for the ECA model, the $F_{95\%}(dof_1, dof_2)$ and $\chi^2_{dof_1,95\%}$ values are 271.76 and 1.1997 respectively. The last two columns of the table are the ratio of the model and the experimental variances and χ^2 values for each model. The data contradict the goodness of both models, since the ratios of the variances and the χ^2 values are more than the corresponding distribution values. However, the values for the SP model are much less than the values for the ECA model. The other data in the table also verify the ascendancy of the goodness of the fit for the SP model with respect to the ECA model. The computation times to evaluate the voltages at different rates for both models are about 0.001 sec on a Dell Precision T7500, with 2 Quad Core 2.53 GHz Zenon Processors CPUs and 12.285 GB of RAM.

10. ECA model with quadratic R_{ct}

In order to compare the ECA model with the same number of parameters as the SP model, it was assumed that the interfacial charge transfer resistance, R_{ct}, is a linear function of the cell SOC as follows [17]:

$$R^{ch}_{ct} = r^{ch}_0 + r^{ch}_1 SOC_{cell} + r^{ch}_2 SOC^2_{cell}$$
$$R^{dch}_{ct} = r^{dch}_0 + r^{dch}_1 SOC_{cell} + r^{dch}_2 SOC^2_{cell}$$

Thus, the following 10 parameters are required to be estimated:

$$\left\{C, Q, r^{ch}_0, r^{ch}_1, r^{ch}_2, r^{dch}_0, r^{dch}_1, r^{dch}_2, SOC^{ch}_{0,cell}, SOC^{dch}_{0,cell}\right\}$$

Note that the resistance *R* was excluded based on the previous results. The parameters, *t* values and confidence intervals obtained

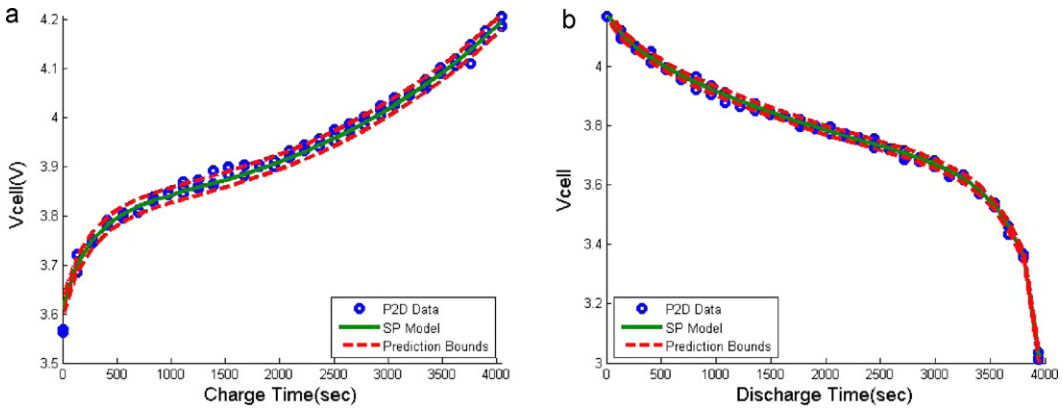

Fig. 7. The fitted SP model with 9 parameters and the prediction bounds for the P2D data (a) 1.0 *C*-rate charge and (b) 1.0 *C*-rate discharge.

Table 10
Statistical results for the P2D data fitting using the ECA model.

Parameter	6 Parameter model			5 Parameter model				
	Value	*t* value	Is parameter significantly affecting the fitting?	Value	*CI*	*NCI*	*t* value	Is parameter significantly affecting the fitting?
C (F)	21.045	−2201.4	Yes	22.43	±9.6562	±0.43049	−2035.7	Yes
Q (Ah)	2.0764	122.54	Yes	2.086	±0.030784	±0.014757	133.5	Yes
R (Ω)	0.029635	1.2631	No	–	–	–	–	–
R_{ct} (Ω)	0.010328	0.45509	No	0.038705	±0.0077621	±0.20054	9.8237	Yes
SOC_{cell}^{ch}	0.91685	123.19	Yes	0.91262	±0.013383	±0.014664	134.35	Yes
SOC_{cell}^{dch}	0.037124	6.1923	Yes	0.041068	±0.010204	±0.24846	7.9294	Yes

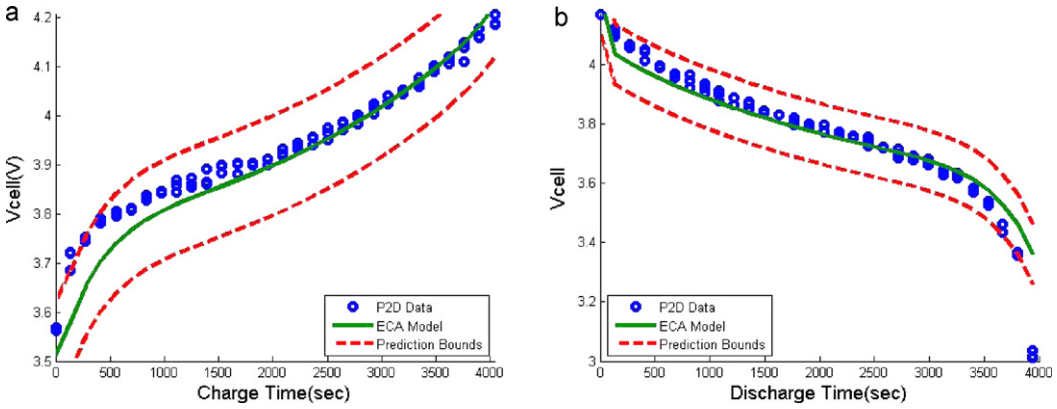

Fig. 8. The fitted ECA model with 5 parameters and the prediction bounds for the P2D data (a) 1.0 *C*-rate charge and (b) 1.0 *C*-rate discharge.

Table 11
Statistical results for the Quallion data fitting using the ECA model with quadratic R_{ct}.

Parameter	10 Parameter model			8 Parameter model				
	Value	*t* value	Is parameter significantly affecting the fitting?	Value	*CI*	*NCI*	*t* value	Is parameter significantly affecting the fitting?
C (F)	75.467	−324.51	Yes	48.68	±38.864	±0.79835	−508	Yes
Q (Ah)	3.0363	191.01	Yes	3.0462	±0.031447	±0.010324	192.18	Yes
r_0^{ch} (Ω)	0.10065	3.2704	Yes	0.1078	±0.035978	±0.33376	5.9443	Yes
r_1^{ch}	0.0010993	0.012323	No	–	–	–	–	–
r_2^{ch}	−0.07627	−0.77127	No	–	–	–	–	–
r_0^{dch} (Ω)	0.21198	31.033	Yes	0.20728	±0.01439	±0.069423	28.578	Yes
r_1^{dch}	−8.6635	−13.777	Yes	−7.9307	±1.2142	±0.1531	−12.959	Yes
r_2^{dch}	10.594	13.18	Yes	9.7004	±1.678	±0.17298	11.469	Yes
SOC_{cell}^{ch}	0.095094	5.0206	Yes	0.069774	±0.035081	±0.33376	3.946	Yes
SOC_{cell}^{dch}	0.7955	191.01	Yes	0.79291	±0.0081856	±0.069423	192.18	Yes

for Quallion data fitting are presented in Table 11 that indicates that the linear and quadratic coefficients for the charge R_{ct} does not affect the fitting significantly. Thus, the charge R_{ct} was kept constant for the subsequent estimation. The R_{ct} linear coefficient at discharge (r_1^{dch}) makes the resistance take negative values at some cell SOC. In this condition a small positive value (e.g. 1e−6) is used for the resistance. Other statistical quantities are given in Table 5 that shows the improvement of the ECA model. However, the SP model is still superior to the ECA model.

11. Conclusion

The reliability of the physics-based SP model to predict the voltage data under different constant current charges and discharges has been compared to the semi-empirical ECA model. The nonlinear least squares approach was used to estimate the parameters of the models by minimizing the *SSE* between the model prediction and the data. In order to enhance the probability of finding the best fit, the genetic algorithm was also implemented to check the optimality of the solution obtained by the trust region method. The statistical *t*-test was accomplished to determine the significant parameters of the models. For the SP model, the cathode diffusion coefficient did not influence the fitting for all data sets. The anode diffusion coefficient for the Quallion data and the anode reaction rate constant for the USG data were not the significant parameters. The resistance R had no strong effect of the fitting for the ECA model for all data sets. Comparing the statistical results demonstrated that the SP model fit all the data sets more precisely (less *SSE*, *RMSE*, *more* R^2, AR^2) and more confidently (tighter prediction bounds) than the ECA model. On other hand, the SP model's computation time to evaluate the voltages is as the same order of magnitude as the ECA computation time. Thus, the SP model is the superior candidate model rather than the ECA model and it can be applied for the online estimation of the SOC and the state of the health of the battery packs. However, based on the assumptions of the SP model and semi-empiricalness

of the ECA model, both models might be inaccurate at high rates where the solution phase resistance cannot be ignored for the SP model, and more electrical components for the ECA would be required. The other limitation of the present models is the incapability of prediction of the cell capacity fade. Thus, some extensions (more terms and/or parameters' dependence on SOC or time, etc.) to the current models are essential to overcome the restrictions.

References

[1] M. Doyle, T.F. Fuller, J. Newman, J. Electrochem. Soc. 140 (1993) 1527.
[2] T.F. Fuller, M. Doyle, J. Newman, J. Electrochem. Soc. 141 (1994) 1.
[3] M. Doyle, J. Newman, J. Electrochem. Soc. 143 (1996) 1890.
[4] R. Darling, J. Newman, J. Electrochem. Soc. 145 (1998) 990.
[5] P. Ramadass, B. Haran, R.E. White, B.N. Popov, J. Power Sources 123 (2003) 230.
[6] C.Y. Wang, W.B. Gu, B.Y. Liaw, J. Electrochem. Soc. 145 (1998) 3407.
[7] V.R. Subramanian, D. Tapriyal, R.E. White, Electrochem. Sol. State Lett. 7 (9) (2004) A259–A263.
[8] M. Ozisik, Boundary Value Problems of Heat Conduction, Dover Publications, NY, 1968.
[9] B.S. Haran, B.N. Popov, R.E. White, J. Power Sources 75 (1998) 56.
[10] G. Ning, B.N. Popov, J. Electrochem. Soc. 151 (2004) A1584.
[11] S. Santhanagopalan, Q. Guo, R.E. White, J. Electrochem. Soc. 154 (2007) A198–A206.
[12] S. Santhanagopalan, Q. Guo, P. Ramadass, R.E. White, J. Power Sources 156 (2006) 620.
[13] I. Bloom, B.W. Cole, J.J. Sohn, S.A. Jones, E.G. Polzin, V.S. Battaglia, G.L. Henriksen, C. Motloch, R. Richardson, T. Unkelhaeuser, D. Ingersoll, H.L. Case, J. Power Sources 101 (2001) 238.
[14] B.Y. Liaw, R.G. Jungst, G. Nagasubramanian, H.L. Case, D.H. Doughty, J. Power Sources 140 (2005) 157.
[15] M. Schlesinger, Modern Aspects of Electrochemical, No. 43, Modeling and Numerical Simulation.
[16] I.J. Ong, J. Newman, J. Electrochem. Soc. 146 (1999) 4360.
[17] M.W. Verbrugge, R.S. Conell, J. Electrochem. Soc. 149 (2002) A45–A53.
[18] M.W. Verbrugge, E. Tate, J. Power Sources 126 (2004) 236.
[19] M.W. Verbrugge, P. Liu, S. Soukiazian, J. Power Sources 141 (2005) 369.
[20] M.W. Verbrugge, B. Koch, J. Electrochem. Soc. 153 (2006) A187–A201.
[21] L. Gao, S. Liu, R.A. Dougal, IEEE Transactions on components and packaging technologies, 25, No. 3.
[22] M. Dubarry, N. Vuillaume, B.Y. Liaw, J. Power Sources 186 (2009) 500.
[23] A.J. Bard, L.R. Faulkner, Electrochemical Methods: Fundamentals and Applications, Wiley, New York, USA, 1980.
[24] M.W. Verbrugge, in: M. Schlesinger (Ed.), Modern Aspects of Electrochemistry, Modeling and Numerical Simulations I, vol. 43, Springer, New York, 2009.
[25] http://www.mathworks.com/.
[26] A. Constantinides, N. Mostoufi, Numerical Methods for Chemical Engineers with MATLAB Applications, Prentice Hall, Upper Saddle River, NJ, 1999.
[27] Curve Fitting Toolbox For Use with MATLAB®.
[28] R.E. Walpole, R.H. Myers, S.L. Myers, K. Ye, Probability & Statistics for Engineers and Scientists, Prentice Hall, Upper Saddle River, NJ, 2002.
[29] K. Kumaresan, G. Sikha, E. Ralph, White, J. Electrochem. Soc. 155 (2008) A164–A171.
[30] H. Yang, J. Prakash, J. Electrochem. Soc. 151 (2004) A1222–A1229.
[31] L. Cai, R.E. White, Mathematical modeling of a lithium ion battery with thermal effects in COMSOL Inc. Multiphysics (MP) software, J. Power Sources 196 (2011) 5985–5989.